

## Rho-mediated regulation of tight junctions during monocyte migration across the blood-brain barrier in HIV-1 encephalitis (HIVE)

Yuri Persidsky, David Heilman, James Haorah, Marina Zelivyanskaya, Raisa Persidsky, Gregory A. Weber, Hiroaki Shimokawa, Kozo Kaibuchi, and Tsuneya Ikezu

**The blood-brain barrier (BBB) is compromised during progressive HIV-1 infection, but how this occurs is incompletely understood. We studied the integrity of tight junctions (TJs) of brain microvascular endothelial cells (BMVECs) in an in vitro BBB system and in human brain tissues with HIV-1 encephalitis (HIVE). A down-regulation of TJ proteins, claudin-5 and occludin, paralleled monocyte migration into the brain during HIVE. Because small G proteins (such as Rho) can play a role in BMVEC TJ assembly, an artificial BBB**

**system explored the relationship among TJs, Rho/Rho kinase (RhoK) activation, and transendothelial monocyte migration. Coculture of monocytes with endothelial cells led to Rho activation and phosphorylation of TJ proteins. Rho and RhoK inhibitors blocked migration of infected and uninfected monocytes. The RhoK inhibitor protected BBB integrity and reversed occludin/claudin-5 phosphorylation associated with monocyte migration. BMVEC transfection with a constitutively active mutant of RhoK led to**

**dislocation of occludin from the membrane and loss of BMVEC cell contacts. When dominant-negative RhoK-transfected BMVECs were used in BBB constructs, monocyte migration was reduced by 84%. Thus, loss of TJ integrity was associated with Rho activation caused by monocyte brain migration, suggesting that Rho/RhoK activation in BMVECs could be an underlying cause of BBB impairment during HIVE. (Blood. 2006;107:4770-4780)**

© 2006 by The American Society of Hematology

### Introduction

HIV-1-associated dementia (HAD) is characterized by cognitive, behavioral, and motor abnormalities affecting up to 11% of infected individuals in the era of highly active antiretroviral therapy.<sup>1</sup> Clinical disease is often correlated with HIV-1 encephalitis (HIVE) and characterized by monocyte brain infiltration, productive infection of brain macrophages and microglia, giant cell formation, myelin pallor, astrogliosis, and neuronal injury.<sup>2</sup> The best histopathologic correlate of HAD is the number of inflammatory macrophages that accumulate in affected brain tissue.<sup>3</sup> This concept is further supported by more recent data demonstrating the importance of perivascular macrophages as viral reservoirs and perpetrators of disease.<sup>4,5</sup> It is now widely accepted that HAD neuronal dysfunction and death are caused by monocyte/macrophage secretory products and viral proteins.<sup>6-13</sup> These observations strongly suggest that monocyte migration across the blood-brain barrier (BBB) is a pivotal event in disease.

BBB compromise is associated with HAD. Examination of HIVE brain tissue reveals that expression of tight junctions ([TJs] providing structural integrity) decreases on brain microvascular endothelial cells (BMVECs).<sup>14,15</sup> HIV-1 patients exhibit signs of BBB compromise by neuroimaging studies.<sup>16,17</sup>

Structurally, the BBB is composed of specialized nonfenestrated BMVECs connected by TJs in an impermeable monolayer

devoid of transcellular pores.<sup>18</sup> TJs are composed of claudins and occludin (integral membrane proteins) and intracellular proteins, zonula occludens (ZO-1, ZO-2, ZO-3).<sup>19</sup> TJs formed by BMVECs maintain the structural integrity of the BBB, limiting paracellular passage of molecules and cells into the brain. Formation of TJs depends on the expression of high levels of occludin and claudin-5 and intracellular signaling processes that control phosphorylation of junctional proteins.<sup>19,20</sup> A recent study demonstrated that claudin-5 is a critical determinant of BBB permeability in mice.<sup>21</sup> The functional significance of occludin as compared with claudin-5 at TJs is not clear. Although claudin-5 is now considered to be the most important TJ protein, it is also expressed on endothelium of less tight barriers while occludin is detected principally in brain endothelial cells with TJs.<sup>22</sup>

TJs are dynamic structures that readily adapt to a variety of physiologic or pathologic circumstances.<sup>23</sup> However, the precise mechanism(s) through which they operate is still unclear. It is widely accepted that F-actin filaments found at the TJ participate in TJ regulation,<sup>24</sup> and actin may be linked to occludin/claudins through ZO proteins.<sup>25,26</sup> While significant progress has been made in identification of the molecular mechanisms that attract leukocytes from the blood and promote their arrest on the vessel wall, less is known about the migration of leukocytes through endothelial cytoplasm or cell-to-cell borders

From the Center for Neurovirology and Neurodegenerative Disorders, Department of Pathology and Microbiology, Pharmacology and Experimental Neuroscience, University of Nebraska Medical Center, Omaha; Department of Cardiovascular Medicine, Tokohu University Graduate School of Medicine, Sendai, Japan; and Department of Cell Pharmacology, Nagoya University Graduate School of Medicine, Aichi, Japan.

Submitted December 2, 2005; accepted January 30, 2006. Prepublished online as *Blood* First Edition Paper, February 14, 2006; DOI 10.1182/blood-2005-11-4721.

Supported by research grants by the National Institutes of Health (PO1 NS043985, RO1 AA015913, and RO1 MH65151 [Y.P.]; RO1 MH072539 [T.I.])

and a grant from the Pharmaceuticals and Medical Devices Agency (PMDA) in Japan (H.S., K.K.).

An Inside *Blood* analysis of this article appears at the front of this issue.

**Reprints:** Yuri Persidsky, Center for Neurovirology and Neurodegenerative Disorders, Nebraska Medical Center, Omaha, NE 68198-5215; e-mail: ypersids@unmc.edu.

The publication costs of this article were defrayed in part by page charge payment. Therefore, and solely to indicate this fact, this article is hereby marked "advertisement" in accordance with 18 U.S.C. section 1734.

© 2006 by The American Society of Hematology

into tissues.<sup>27-29</sup> Leukocyte migration requires mechanisms that open intercellular junctions, allowing passage of circulating cells and preserving barrier function.<sup>30</sup>

An accumulating body of evidence suggests that small G proteins such as Rho play a role in BMVEC TJ disassembly through activation of signaling pathways that regulate cytoskeletal organization.<sup>26,31</sup> Given our *in vivo* observations (TJ down-regulation in HIVE) and current understanding of Rho's participation in cytoskeleton alterations in endothelial cells, we hypothesize that BMVEC Rho activation is associated with monocyte brain migration and TJ compromise in HAD. To investigate the role of Rho in monocyte migration across BMVECs, we employed cultures of primary human BMVECs and developed a functional BBB.<sup>32-34</sup> This work investigated whether modulation of Rho alters BMVEC TJ function and whether Rho inhibition in BMVECs prevents monocyte migration across the BBB. Inhibition of the Rho pathway in BMVECs resulted in TJ up-regulation, prevented occludin and claudin-5 phosphorylation (induced by monocytes), and diminished monocyte transendothelial migration. Rho signaling in BMVECs likely plays a crucial role in monocyte migration across the BBB and in TJ assembly, all relevant to the neuropathogenesis of HIV-1 infection.

## Materials and methods

### Monocyte isolation, propagation, and viral infection

Peripheral-blood mononuclear cells were obtained from HIV-1-, HIV-2-, and hepatitis B-seronegative donors by leukopheresis and then purified by counter current centrifugation to generate pure populations of monocytes.<sup>35</sup> Monocytes were infected with HIV-1<sub>ADA</sub> at a multiplicity of infection of 0.1 virus/target cell for 18 hours.<sup>35</sup> Prior to infection, the HIV-1 cellfree stocks were treated with DNase I for 30 minutes at 37°C as described.<sup>36</sup> All reagents were prescreened for endotoxin (less than 10 pg/mL; Associates of Cape Cod, Woods Hole, MA) and mycoplasma contamination (Gen-Probe II, Gen-Probe, San Diego, CA).

### HIV-1 DNA analysis by polymerase chain reaction (PCR) monocytes

A total of  $2 \times 10^6$  cells per milliliter were cultured in Teflon flasks and infected with HIV-1 as described above. At 8 and 24 hours after infection, the residual medium was washed off with fresh phosphate-buffered saline (PBS) (Sigma, St Louis, MO), and cells were used for the extraction of cellular DNA with the Iso-quick nucleic extraction kit (ORCA Research, Bothell, WA). The DNA was resuspended at a concentration of  $10^4$  cell equivalents per microliter. PCR was performed to identify early (primers to long terminal repeat [LTR] U3/R), intermediate (primers to *pol* I and J regions), and late (primers to LTR U3/*gag*) products of reverse transcription as described previously.<sup>36</sup> Amplified products were hybridized to [<sup>32</sup>Pγ-ATP]-radiolabeled oligonucleotide probes and quantified on a PhosphorImager (Molecular Dynamics, Sunnyvale, CA).<sup>36</sup>

### BMVECs

Primary human BMVECs were isolated from the lateral temporal cortex of brain tissue obtained during surgical removal of epileptogenic foci in adult patients by the procedure described previously<sup>32</sup> and supplied by Dr M. Witte (University of Arizona, Tucson). Routine evaluation for von Willebrand factor (VWF), *Ulex europaeus* lectin, and P-gp demonstrated that cells were more than 99% pure. The procedures have been approved by the University of Nebraska Medical Center (Omaha) institutional review board (IRB).

### BBB models

The BBB models were constructed<sup>32</sup> by placing primary BMVECs ( $25 \times 10^3$  cells) on the upper surface of the membrane of 24-well tissue-culture inserts (Cyclopore polyethylene terephthalate membrane, composed of  $2 \times 10^6/\text{cm}^2$  pores, 3-μm pore diameter; Collaborative Biochemical Products, Becton Dickinson, Franklin Lakes, NJ). The cells were cultured for at least 4 days before use.<sup>32</sup>

### Transendothelial electrical resistance (TEER)

Electrical resistance across the endothelial-cell monolayer was measured by an EVOM voltmeter (World Precision Instruments, Sarasota, FL) as described.<sup>34</sup> Electrical resistance of the blank insert with media alone was subtracted from the TEER from endothelial-cell monolayers. Such a "true" electrical resistance unit was expressed in  $\Omega \text{ cm}^2$  (varied around 380 to 420  $\Omega \text{ cm}^2$  in control/untreated monolayers at the day of experiment). The experiments were independently performed multiple times (each experiment in triplicate), and the results were expressed as mean  $\pm$  SEM from 4 different experiments.

### Transendothelial monocyte migration

A total of  $10^5$  monocytes (with or without HIV-1 infection) was placed in 100 μL medium in the upper chambers of artificial BBB. We used a 1:5 BMVEC/monocyte ratio to minimize nonspecific disruption of the BBB seen in models with higher leukocyte numbers.<sup>28</sup> Under these conditions, *in vitro* BBB is altered modestly (as reflected by TEER), mimicking functional changes in BMVECs. At 0.5, 1, 2, and 6 hours after plating, migrated monocytes were counted in the lower chamber. Human macrophage chemotactic protein-1 (MCP-1) (5 ng/mL; R&D Systems, Minneapolis, MN) in the lower chamber served as a pathophysiologically relevant stimulus, based on our showing before that MCP-1 is up-regulated in HIVE.<sup>33</sup> Migrated monocytes were immunostained with CD68 (macrophage marker, at 1:100 dilution; Dako, Carpinteria, CA). At least 20 random fields (objective  $\times 20$ ) in each well were analyzed for migrated cells (experiments in quadruplicate). Chemotactic responses to MCP-1 varied between different donors of monocytes and ranged from 3- to 7-fold increases of monocyte migration across BBB constructs in response to chemokines compared with controls. Such differences related to individual donor-to-donor variability observed in primary human monocytes. The experiments were independently performed multiple times (at least 4 for all presented data), allowing statistical analyses. In each individual experiment, every condition was evaluated in replicates (3 or 4).

### Rho and RhoK inhibition in BMVECs

To explore the role of Rho and RhoK inhibition in BMVECs during monocyte migration, Rho inhibitor (*Clostridium botulinum* C3 transferase, 10 or 50 μg/mL; Sigma) or RhoK inhibitor (Y-27632, 10 μM; Calbiochem, San Diego, CA) was applied to the upper chamber and then removed by washing before addition of monocytes to the upper chamber. Alternatively, replicate monocytes were pretreated with C3 transferase or Y-27632 before introduction to the upper chamber.

### Cell culture and extraction

Brain endothelial cells were cultured in T75 flasks ( $3 \times 10^6$  per flask). Upon 100% confluency (about  $5 \times 10^6$  cells per flask), endothelial cells were cocultured with monocytes for 1 or 2 hours at 37°C (at the ratio of 1:5 BMVECs/monocytes). Part of the endothelial-cell population was preincubated with RhoK inhibitor (Y-27632, 10 μM for 2 hours at 37°C) before monocyte application. Cells were extracted by scraping the monolayer in the same culture media, followed by centrifugation at 850g for 5 minutes at 4°C. Cell pellets (transferred into 1.5-mL tubes) were washed twice with ice-cold  $1 \times$  PBS and were lysed with 1.0 mL ice-cold lysis buffer (10 mM Tris-HCl [pH 7.4] containing 20% glycerol, 0.5% Triton X-100, 100 mM NaCl<sub>2</sub>, and protease inhibitor cocktail). Lysates were centrifuged at 14 000g for 10 minutes at 4°C to clear cell debris. The supernatants were used for affinity precipitation or for immunoprecipitation assays.

### Affinity precipitation of Rho-GTP

Rho-GTP (the active form of Rho) was isolated from lysates by an affinity precipitation technique using EZ-Detect Rho activation kit from Pierce (Rockford, IL). In brief, one SwellGel immobilized glutathione disc resin for each lysate was placed in a spin column with a collection tube. A total of 400  $\mu$ g GST-rhotekin-RBD protein and 400  $\mu$ g lysate proteins from respective samples were added to each tube and incubated for 1 hour at 4°C with gentle agitation. The beads were washed 3 times with  $1 \times \text{Mg}^{2+}$  lysis buffer followed by centrifugation at 14 000g for 30 seconds. The beads were then resuspended in 40  $\mu$ L of  $2 \times$  Laemmli sample buffer containing 2- $\beta$ -mercaptoethanol and bromophenol blue for at least 15 minutes. A total of 2  $\mu$ L of 1 M DTT was added to each sample prior to 5 minutes of boiling at 95°C for easy release of Rho-GTP from resin. GTP $\gamma$ S (for positive) and GDP (for negative) supplied by Pierce were used as respective controls.

### Immunoprecipitation of occludin and claudin-5

Antioccludin or anti-claudin-5 antibodies (Zymed Laboratories, San Francisco, CA) were covalently conjugated to Affi-Gel 10 resin (Bio-Rad, Hercules, CA), and immunoprecipitation was performed as described.<sup>34</sup>

### Western blot assays

Duplicate immunoprecipitation samples of 20  $\mu$ L each were loaded to 2 separate 12% precast polyacrylamide gels; one was used for detection of serine-phosphorylated, tyrosine-phosphorylated, or threonine-phosphorylated occludin/claudin-5 and the other for total occludin/claudin-5 analysis. The gels were subjected to electrophoresis, transferred onto nitrocellulose membranes, and the membranes probed with primary antibodies to occludin (for total occludin), claudin-5 (total claudin-5), or antibodies to phosphoserine, phosphotyrosine, or phosphothreonine (phosphorylated occludin/claudin-5) (all purchased from Zymed).

Samples of 40  $\mu$ L each from glutathione affinity precipitation (GTP active form of Rho) or 10  $\mu$ g nonprecipitated cell lysate (active and inactive form of Rho) were loaded onto a 1.5 mm-thick precast 12% polyacrylamide gel for Western blotting. The membranes were blocked with Superblock (Pierce) for 1 hour at room temperature followed by membrane incubation with primary polyclonal anti-Rho antibodies (3  $\mu$ g/mL). After washing 2 times, membranes were incubated with the appropriate secondary antibody for 1 hour at room temperature. The immunoreactive bands were detected with Luminol detection kits (Pierce), followed by exposure to Kodak x-ray film (Eastman Kodak, Rochester, NY). The bands were quantified densitometrically as arbitrary volume integration units (VIU) using Image-Quant software (Molecular Dynamics, Sunnyvale, CA). Results were corrected for the internal standard  $\alpha$ -actin for active Rho-GTP and the total Rho (active and inactive Rho). Similarly, the phosphorylated occludin/claudin-5 and total occludin/claudin-5 were expressed as the ratio to internal standard  $\alpha$ -actin.

### DNA transfection

Dominant active RhoK (DA-RhoK) was originally named pEF-BOS-Myc-CAT, and dominant negative RhoK (DN-RhoK) was named pEF-BOS-Myc-RB/PH (TT).<sup>37</sup> These constructs express a c-Myc-tagged recombinant molecule under the control of the elongation factor-1 (EF-1) promoter. Endothelial cells were cultured in T25 flasks (at  $1.5 \times 10^6$  cells per flask) or 4-well Lab-Tek Chamber Slide (Nunc, Rochester, NY) (at 30 000 cells per well), which were coated with collagen-fibronectin prior to the cell culture. Twenty-four hours after plating, 0.3  $\mu$ g plasmids (DA- or DN-RhoK) were transfected by culture with 2.4  $\mu$ L GenePorter II (Gene Therapy Systems, San Diego, CA) in 300  $\mu$ L DMEM without serum or antibiotics overnight according to the manufacturer's protocol. The media were aspirated, and fresh endothelial culture media were added. At days 3, 5, 7, 9, and 11 after DNA transfection, cells were washed and fixed with 4% paraformaldehyde in PBS for 20 minutes and washed 5 times with PBS. The slides were evaluated by immunofluorescence for expression of TJ molecules and

recombinant molecules using anti-Myc monoclonal Ab (9E10,1:100; Santa Cruz Biotechnology, Santa Cruz, CA). For BBB constructs, BMVECs were cultured at a density of 30 000 cells per well in 24-well Transwells (Becton Dickinson) that were coated with collagen-fibronectin prior to the cell culture and transfected similarly with plasmids. At days 2, 3, and 5 after DNA transfection, monocytes were applied to upper chambers for the migration studies.

### Recombinant adenovirus

DN-RhoK adenovirus, which expresses c-Myc-tagged DN-RhoK (RB/PH(TT)) under the control of a cytomegalovirus (CMV) promoter with enhanced green fluorescent protein (EGFP) as a separate tracer, was originally named AdDNRhoK.<sup>38</sup> We used the control adenovirus (R-CON), which expresses GFP under the control of the CMV promoter but without DN-RhoK.<sup>39</sup> The viruses were amplified by repeated infection into human embryonic kidney (HEK) 293 cells, followed by purification using CsCl banding as described.<sup>39</sup> The purified virus was used at  $3 \times 10^6$  expression-forming units per milliliter for infecting  $3 \times 10^4$  cells in 4-well Lab-Tek Chamber Slide or Transwell inserts in the endothelial-cell culture media overnight, followed by washing twice with DMEM and incubation with fresh culture media. The expression of recombinant molecules was monitored by EGFP/GFP signal under a Nikon TE-300 inverted fluorescent microscope (Nikon, Melville, NY). The infected cells were used for immunofluorescence or migration studies at days 2, 3, and 5.

### Immunofluorescence microscopy

BBB membranes, adherent cultures of BMVECs, or frozen human brain sections were immunolabeled with antibodies directed against occludin (mouse IgG or rabbit IgG, 1:100; Zymed), claudin-5 (mouse IgG, 1:100; Zymed), ZO-1 (rabbit IgG, 1:100; Zymed), HAM-56 (macrophage marker, mouse IgM, 1:100; Dako), GFAP (astrocyte marker, mouse IgG, 1:100; Dako), VWF (endothelial-cell marker, rabbit IgG, 1:100; Dako), and *U europaeus* lectin (endothelial-cell marker, 1:100; Dako). Samples were incubated with primary antibodies for 2 hours at room temperature or overnight at 4°C and then probed with secondary antibodies coupled with Alexa-488 (1:100; Molecular Probes, Eugene, OR), Alexa-568 (1:100; Molecular Probes), TRITC, or rhodamine (1:100; Dako) for 1 hour at room temperature. Cells were stained with rhodamine-phalloidin (1:1000; Molecular Probes) to visualize F-actin. Stained monolayers, BBB constructs, or frozen human brain sections were mounted with Immunomount (Molecular Probes) and examined using a Nikon E800 fluorescence microscope connected to a color MagnaFire digital camera (Optronics, Goleta, CA). Laser confocal microscopy was performed using a Zeiss LSM410 argon/krypton dual-beam confocal laser scanning microscope (CLSM) connected to a Zeiss microscope (Zeiss, Thornwood, NY).

### Scanning electron microscopy (SEM)

For SEM, specimens were processed as described<sup>32</sup> and examined with a Hitachi-F 3000N scanning electron microscope (Hitachi High Technologies America, Pleasanton, CA).

### Human brain tissue

Frontal cortex and basal ganglia specimens were derived from 6 HIVE cases of different severity (4 severe, 2 moderate, and 2 mild according to previously described criteria<sup>33</sup>). Brains from 4 HIV-1-positive patients without evidence of encephalitis and from 5 seronegative age-matched controls were provided by the National NeuroAIDS Consortium (Washington, DC) and the brain bank of the Center for Neurovirology and Neurodegenerative Disorders (Table 1). Approval was obtained from the University of Nebraska Medical Center IRB for these studies. Serial frozen sections (5- $\mu$ m thickness) were cut and double immunostained (indirect immunofluorescence) for occludin/HAM56, claudin-5/HAM56, occludin/phosphoserine, or occludin/phosphothreonine as described.<sup>33</sup> Paraffin sections (5- $\mu$ m thickness) were cut and double immunostained (immunoperoxidase technique) for claudin-5 and CD163 (marker of monocytes and

**Table 1. Human brain tissues: clinical and pathologic description**

Case	Neuropathologic alterations	Proportion of microvessels with disrupted occludin and claudin-5 immunostaining, %
1	Severe HIVE*	54
2	Severe HIVE	45
3	Severe HIVE	60
4	Severe HIVE	60
5	Moderate HIVE†	45
6	Moderate HIVE	50
7	Mild HIVE‡	15
8	Mild HIVE	20
9	HIV-1§	2
10	HIV-1	0
11	HIV-1	0
12	HIV-1	0
13	Control	0
14	Control	0
15	Control	0
16	Control	0
17	Control	0

\*Severe HIVE is defined as expression of HLA-DR on 80% to 90% of microglia; HIV-1 infection of ramified microglia; formation of 1 to 2 microglial nodules and 25 to 50 infiltrating macrophages per five  $\times$  10-power fields; and abundant multinucleated cells.

†Moderate HIVE is defined as expression of HLA-DR on 20% to 70% of microglia; formation of 1 to 2 microglial nodules per ten  $\times$  10-power fields and 5 to 25 infiltrating macrophages per five  $\times$  10-power fields; and frequent multinucleated giant cells.

‡Mild HIVE is defined as expression of HLA-DR on 10% to 15% of microglia; 1 microglial nodule per twenty  $\times$  10-power fields and 3 to 5 CD68<sup>+</sup> infiltrating macrophages per five  $\times$  10-power fields; and rare multinucleated cells (as described before<sup>33</sup>).

§HIV-1-seropositive patients who died of complications of AIDS not related to the CNS; no changes were seen on neuropathologic examination.

perivascular macrophages, mouse IgG, 1:100; Vector Laboratories, Burlingame, CA) as described.<sup>40</sup>

### Statistical analyses

All results were expressed as mean  $\pm$  SEM. One-way analyses of variance (ANOVA) were used to compare mean responses among experimental groups, and the Newman-Keuls posttest was used to determine significance between groups (using GraphPad Prism 2.0; GraphPad Software, San Diego, CA).

## Results

### Monocyte migration across the BBB disrupts TJs in vivo and in vitro

To investigate whether TJs are disrupted in HIVE, we examined changes in occludin and claudin-5 expression in 6 cases of HIVE, 4 brains from HIV-1 seropositive patients without encephalitis, and 5 brains from virus-seronegative controls. Double immunostaining for occludin or claudin-5 (green) and the monocyte/macrophage marker (HAM-56, red) demonstrated continuous occludin and claudin staining in control brains (Figure 1A,D) and HIV-1-seropositive cases. However, microvessels featuring monocyte migration across the BBB demonstrated disrupted staining in HIVE (Figure 1B-C,E-F). Further, the decrease in occludin and claudin immunostainings was associated with the level of monocyte brain infiltration (HIVE with mild monocyte infiltration [Figure 1B,E]; HIVE with intense monocyte infiltration [Figure 1C,F]). Double immunostaining for claudin (brown) and CD163 (marker for monocytes/macrophages, purple) showed uniform continuous staining of TJ protein and rare perivascular macrophages in control brain tissue (Figure 2A,F), while 45% to 60% of microvessels demonstrated disrupted claudin-5 immunostaining in severe and moderate HIVE (Figure 2B-D) as compared with 15% to 20% of the microvessels in mild HIVE (Figure 2E; Table 1). These changes were not detected in brains from HIV-1-seropositive patients without encephalitis and from virus-seronegative controls. Laser confocal microscopy of HIVE brain tissue demonstrated that monocyte infiltration (HAM-56, red) occurred between TJs (claudin-5; Figure 1G, green, arrow). These data support the idea that disruption of TJs (both occludin and claudin-5) occurs during monocyte migration into the brain, and monocyte passage appears to occur between TJs.

To explore the mechanisms of BBB disruption shown in prior pathologic examinations, we used primary human BMVECs isolated from normal brain tissue during neurosurgical removal of epileptogenic foci. Figure 3 demonstrates BMVECs expressing VWF (Figure 3A, endothelial marker) in cytoplasm and the TJ protein, occludin (Figure 3B, arrow), at cell borders. Our previous studies demonstrated that these cells are connected by TJs.<sup>32</sup>

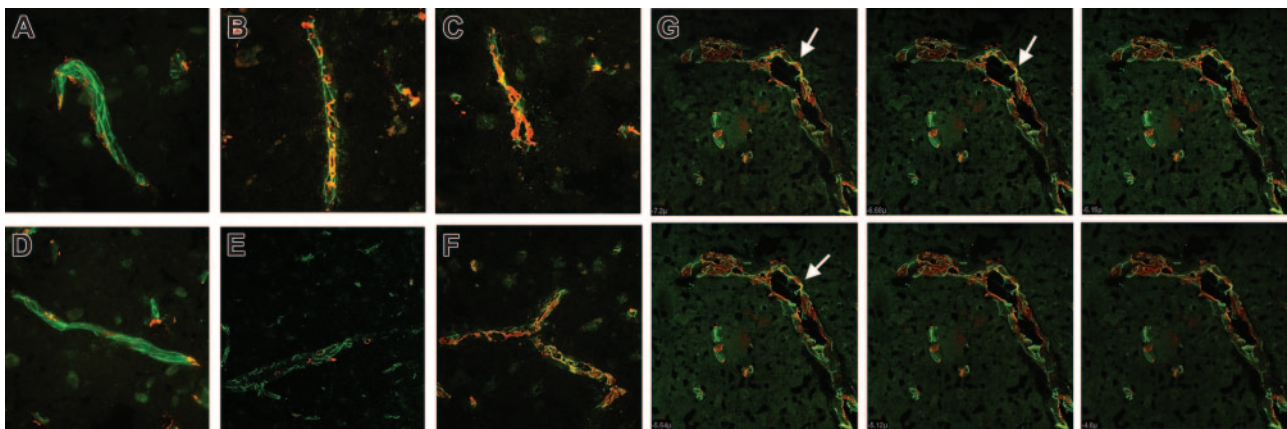


**Figure 1. TJ alterations in brain tissue with HIVE.** Microvessels from control brain showed intact and continuous TJs (occludin, green [A]; claudin-5, green [D]) and few perivascular macrophages (HAM-56, red [A,D]). Microvessels in areas of intensive monocyte migration (HAM-56, red) seen in HIVE featured fragmented/weak immunoreactivity for occludin (green [B-C]) and claudin-5 (green [E-F]). (G) Monocytes (HAM-56, red) migrating between borders of brain endothelial cells expressing claudin-5 (green, arrow) in human brain tissue affected by HIVE. Serial z-sectioning (0.52- $\mu$ m interval) was performed using a Zeiss LSM410 argon/krypton dual-beam CLSM connected to a Zeiss microscope. (A-G) Original magnification,  $\times$  200. Images were visualized using a 20  $\times$ /0.5 numerical aperture (NA) objective and were acquired using a Color View II digital charge-coupled device (CCD) camera (Soft Imaging Systems, Lakewood, CO).

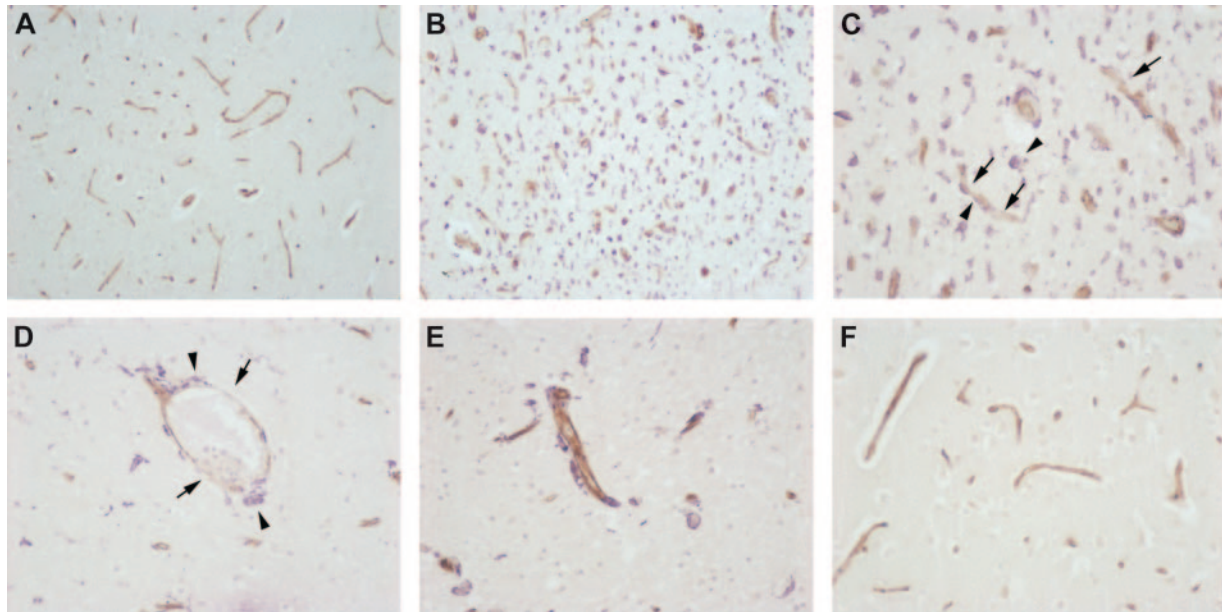


**Figure 2. TJ alterations correlated with monocyte infiltration in brain tissue with HIVE.** Microvessels from control brain showed intact and continuous TJs (claudin-5, brown) and rare perivascular macrophages (CD163, purple [A,F]). Decreased staining for claudin-5 (arrows) was seen in microvessels in areas of intensive monocyte migration (arrowheads) in severe (B-C) and moderate (D) HIVE. Brain tissue with mild HIVE demonstrated little changes in claudin-5 staining (brown) and perivascular macrophages (CD163, purple [E]). Original magnification (A-B)  $\times 100$ ; (C-F)  $\times 200$ . Images were visualized using a  $10\times/0.3$  NA (A-B) or a  $20\times/0.5$  NA (C-F) objective and were acquired using a Color View II digital CCD camera.

Monocytes cocultured with BMVECs for 0.5 to 2 hours resulted in the relocation of occludin from cellular borders into the cytoplasm (Figure 3C, arrow), suggesting the disassembly of TJs during monocyte-BMVEC interactions. We next examined actin distribution in BMVECs. Endothelial cells demonstrated a rim of F-actin staining at the periphery of cytoplasm. Monocyte-BMVEC interactions resulted in progressive actin polymerization (from 10 to 60 minutes) with formation of stress fibers within the cytoplasm (data not shown). Importantly, changes in actin cytoskeleton paralleled dislocation of occludin staining from cellular borders to cytoplasm.

To determine whether the cell borders occupied by TJs serve as a focal point for monocyte migration, we added freshly isolated monocytes to the artificial BBB constructs. The BBB system (TEER,  $400\ \Omega\ \text{cm}^2$ ) without monocytes showed a flat surface without gaps between endothelial cells (Figure 2D). Monocytes applied to the BBB attached to endothelial-cell borders (Figure 2E) and migrated across the BBB between cell borders (Figure 2F). Prominent monocyte migration in response to MCP-1 (up-regulated in human brain tissue affected by HIVE) led to focal retraction and formation of small gaps. We assume that such changes develop during massive monocyte infiltration in vivo (as seen in Figures 1C,F and 2B,D).

#### Rho inhibitor prevents migration of HIV-1-infected monocytes

Possible links between Rho activation and monocyte migration was next studied. Application of uninfected or infected monocytes to brain endothelial cells resulted in a significant increase of the active form of Rho (Rho-GTP) (Figure 4A-B). While Rho-GTP was increased more than 2-fold ( $P < .01$ ) in cocultured BMVECs/monocytes and BMVECs/HIV-1 monocytes as compared with endothelial cells alone, total Rho was increased only by 25% to 31% (reflecting contribution of monocyte Rho) when equal amounts of protein were used for each condition (Figure 4C).

To investigate inhibition of Rho activity in BMVECs versus Rho derived from monocytes in coculture, we pretreated BMVECs with specific Rho inhibitor, *C botulinum* C3 transferase (4 hours;  $50\ \mu\text{g}/\text{mL}$ ), and applied monocytes. After 2-hour coculture, monocytes were washed from BMVECs (allowing removal of more than 90% of applied monocytes) or kept on BMVECs. Again Rho-GTP increased more than 2-fold BMVEC/monocyte coculture ( $P < .01$ ), and monocyte removal only slightly diminished Rho-GTP content (20%,  $P < .01$ ; Figure 4D-F). These data indicated BMVECs were a major contributing factor for the active form of Rho in cocultures. BMVEC treatment with C3 transferase

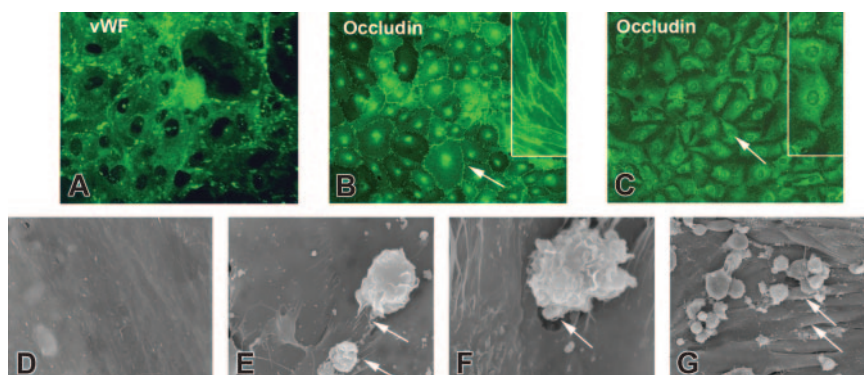


**Figure 3. TJ alterations in BMVECs during coculture with activated monocytes.** Endothelial cells are positive for vWF (A) and express occludin (B, arrow) at cell-cell contacts. Application of monocytes resulted in occludin relocation to cytoplasm (C, arrow). Monocyte migration occurs across TJs in the BBB model. (D) Endothelial cells demonstrate a flat surface without gaps in control BBB constructs (without monocytes). Scanning electron microscopy revealed monocyte attachment to endothelial cell contacts (E, arrows) and their migration between endothelial-cell borders (F, arrow). Massive monocyte migration in response to MCP-1 resulted in focal gap formation of the endothelial monolayer (G). Original magnification (A-C)  $\times 200$ ; (insets, B-C)  $\times 400$ ; (D-E)  $\times 4000$ ; (F)  $\times 7000$ ; (G)  $\times 1200$ . Images were visualized using a  $20\times/0.5$  NA (A-C) or a  $40\times/0.75$  NA (B-C, insets) objective and were acquired using a Color View II digital CCD camera.

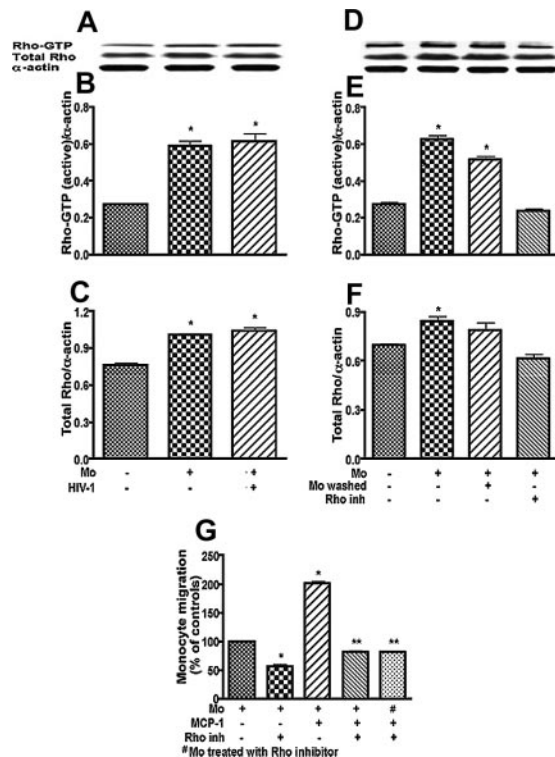


**Figure 4. Coculture of BMVECs with monocytes leads to Rho activation, and Rho inhibitor blocks monocyte migration.** (A-C) The content of both active Rho-GTP and total Rho was measured in BMVECs or BMVECs cocultured with infected or uninfected monocytes for 2 hours. (A) Representative immunoblots of active Rho-GTP, total Rho, and internal standard, actin. (B) Ratio of Rho-GTP/actin. (C) Ratio of total Rho/actin. (D-E) After 2 hours of coculture, monocytes were washed from BMVECs (removing more than 90% of applied monocytes) or kept on BMVECs. The active form of Rho was derived mainly from BMVECs in coculture because monocyte removal slightly diminished Rho-GTP content in protein extracts (bar 2 versus bar 3). Pretreatment of BMVECs with Rho inhibitor, *C botulinum* C3 transferase (4 hours; 50  $\mu$ g/mL), prevented Rho activation in coculture. (D) Representative immunoblots of active Rho-GTP, total Rho, and internal standard, actin. (E) Ratio of Rho-GTP/actin. (F) Ratio of total Rho/actin. Results were expressed as the ratio of target protein immunoreactivity to that of the internal standard, actin. Each bar represents the mean value of 4 replicates  $\pm$  SEM.  $P < .01$  compared with endothelial cells without monocyte coculture. (G) Migration of fresh  $10^5$  monocytes applied to BBB constructs was studied in response to MCP-1 (5 ng/mL in the bottom chamber). Pretreatment of BMVECs in the top chamber with C3 transferase (4 hours; 50  $\mu$ g/mL) diminished monocyte migration across the BBB by 50% (without MCP-1) or 63% (with MCP-1) compared with respective controls. Pretreatment of monocytes with C3 transferase (4 hours; 50  $\mu$ g/mL) resulted in 60% inhibition of migration. Results were normalized to migration of monocytes without MCP-1 (a value of 100%). Values represent the mean of quadruplicate determinations  $\pm$  SEM.  $*P < .01$  compared with BBB constructs without pretreatment and MCP-1 application.  $**P < .01$  compared with BBB constructs with MCP-1 application. Results of 1 representative experiment are shown.

before monocyte application completely blocked Rho activation (Figure 4D-F).

To investigate whether monocyte migration can be blocked by inhibition of Rho, we pretreated the artificial BBB system with *C botulinum* C3 transferase (4 hours or 24 hours; 50  $\mu$ g/mL) to inhibit Rho activities, and BBB constructs were washed before monocyte application. Human monocytes were placed onto the endothelial chamber, and MCP-1 applied to the lower chamber resulted in more than a 2-fold increase in monocyte migration (Figure 4G). Pretreatment of the BBB with C3 transferase efficiently blocked migration of monocytes across the BBB both in the absence (50% decrease,  $P < .01$ ) or presence of MCP-1 (63% inhibition,  $P < .001$ ) as compared with untreated controls (Figure 4G). Because Rho was suggested to play an important role in monocyte migration,<sup>41</sup> we used monocytes pretreated with C3 transferase as an additional control in our system. Importantly,

pretreatment of monocytes with C3 transferase (4 hours; 50  $\mu$ g/mL) before application to BBB constructs also diminished monocyte migration (62% inhibition,  $P < .001$ ). The results of these experiments (repeated 4 times with BMVECs derived from 3 different donors) suggested that monocyte migration could be efficiently blocked by inhibition of a Rho signaling pathway.

To mimic the HIV pathologic process, we investigated the effects of Rho inhibition on the migration of HIV-1-infected monocytes across the BBB. Freshly elutriated monocytes were exposed to HIV-1 for 18 hours. At this time point, early and late products of reverse transcription are present (Figure 5A). Monocytes were placed into the endothelial chamber, and MCP-1 was applied to the lower chamber in replicate wells. HIV-1-infected monocytes demonstrated an enhanced ability to migrate across the BBB constructs as compared with uninfected cells (33%) in response to MCP-1 (Figure 5B, bars 2 and 6). Rho inhibitor (C3 transferase; 24 hours; 10  $\mu$ g/mL; applied in replicate wells and then washed before monocyte application) efficiently blocked the migration of both uninfected and HIV-1-infected cells by 25% and 40%. C3 transferase pretreatment of the BBB resulted in random distribution of F-actin filaments in BMVECs and the absence of stress fiber formation after monocyte application to BBB constructs. Again, monocyte treatment with Rho inhibitor before application to BBB constructs was used as an additional functional control. Thus, Rho inhibition in both BMVECs and monocytes may block monocyte migration across the BBB.

#### DN-RhoK expression in BMVECs diminishes monocyte migration

RhoK is a downstream enzyme in Rho intracellular signaling. To further explore the role of Rho signaling pathways in BMVEC TJ

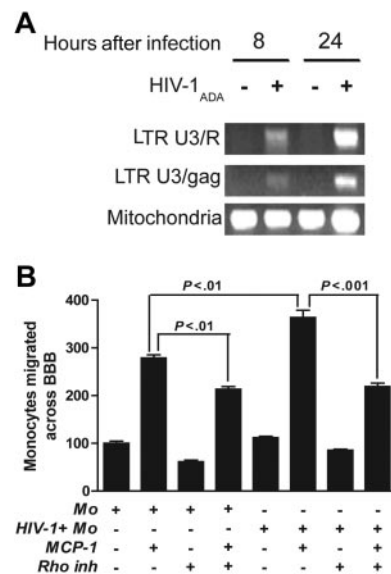


**Figure 5. Rho inhibitor blocks migration of HIV-1-infected monocytes.** (A) Cells were infected with HIV-1<sub>ADA</sub> Eight and 24 hours after infection, and cells were lysed for viral DNA analysis. Primers that specifically amplified early and late products of reverse transcription were used. The PCR-amplified products were quantified on a PhosphorImager after hybridization. A representative experiment is shown. (B) HIV-1-infected (18 hours after infection) or uninfected monocytes ( $10^5$ ) were applied to BBB constructs, and their migration was studied in response to MCP-1 (5 ng/mL in the bottom chamber). Pretreatment of the top-chamber BMVECs with *C botulinum* C3 transferase (24 hours; 10  $\mu$ g/mL) diminished migration of infected and uninfected cells by 40% and 25%, respectively, across the BBB. Results were normalized to migration of uninfected monocytes without MCP-1 (a value of 100%). Values represent the mean of quadruplicate determinations  $\pm$  SEM. Results of 1 representative experiment are shown.

assembly, BMVECs were virally transfected with recombinant DN-RhoK adenoviral construct, which coexpresses EGFP.<sup>38</sup> BMVEC transfection, as evidenced by expression of EGFP by 70% to 80% of BMVECs, occurred by 48 hours after viral application and resulted in overexpression of occludin in BMVEC cellular contacts. When DN-RhoK-transfected BMVECs were used to assemble the BBB constructs, a significant reduction in monocyte migration (35%,  $P < .001$ ) across the BBB in response to MCP-1 was demonstrated (data not shown). Short-term transfection with R-CON did not alter migration, but a longer period of transfection (more than 72 hours) with R-CON resulted in cytopathic effect and increased levels of monocyte migration.

To confirm our data with the different mode of transfection, we next performed transient transfection of primary human BMVECs with dominant-active RhoK (DA-RhoK) or DN-RhoK mutant.<sup>37</sup> Transfection with DN-RhoK (up to 70% as shown by c-Myc expression; Figure 5A) up-regulated occludin expression (Figure 6B,D,F), while transfection with DA-RhoK resulted in the dislocation of occludin from the membrane and the loss of intercellular contacts (Figure 6C,E). A significant reduction in monocyte migration (84%,  $P < .01$ ) in response to MCP-1 was demonstrated (Figure 6G, bar 6) when DN-RhoK-transfected BMVECs were used to assemble BBB constructs. Monocyte passage through the BBB transfected with DA-RhoK did not differ from control, untransfected cells.

#### RhoK inhibitor prevents phosphorylation of TJs and monocyte migration across the BBB

To investigate a possible link between Rho activation and functional changes of TJ proteins, occludin and claudin-5, we cocultured monocytes with brain endothelial cells and assessed the phosphorylation of occludin and claudin-5 by immunoprecipitation and Western blot analysis of cell lysates using phosphoserine, phosphothreonine, and phosphotyrosine antibodies. One- or 2-hour coculture with uninfected or HIV-1-infected monocytes resulted in increased content of phosphorylated occludin (1.5-fold to 2-fold by uninfected cells and 2-fold to 2.5-fold by HIV-1-infected monocytes,  $P < .01$ ) as compared with endothelial cells cultured alone (Figure 7A-C). Similarly, the amount of phosphorylated claudin-5 increased 2-fold in coculture of BMVECs with uninfected monocytes or 2.5-fold in BMVEC/HIV-1-infected monocytes ( $P < .01$ , Figure 7D-F). Interestingly, infected monocytes caused more pronounced changes in phosphorylation of TJ proteins (20% to 35%,  $P < .01$ ) when compared with uninfected cells. Changes in occludin/claudin-5 phosphorylation paralleled Rho activation (Figure 3A-C). Because part of the downstream signaling of Rho is mediated by RhoK,<sup>42</sup> we pretreated endothelial cells with a highly selective RhoK inhibitor (Y-27632).<sup>43</sup> Treatment of endothelial cells with Y-27632 (10  $\mu$ M for 2 hours) before monocyte application completely reversed claudin-5 phosphorylation and significantly diminished occludin phosphorylation in BMVEC/HIV-1 monocyte coculture (Figure 7A-F). Next, we examined changes in TJ phosphorylation in vivo using human brain tissues described in Table 1 (6 cases of HIVE, 4 HIV-1-seropositive cases without evidence of encephalitis, and 5 seronegative controls). Using double staining for occludin and phosphoserine or phosphothreonine, phosphoserine staining was detected on brain microvessels, which partially overlapped with occludin in HIVE (Figure 7H). No immunostaining for phosphoserine or phosphothreonine was found in controls or brains derived from HIV-1-positive patients without HIVE (Figure 7G). These data indicate that occludin

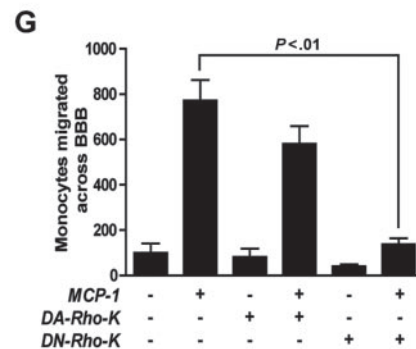
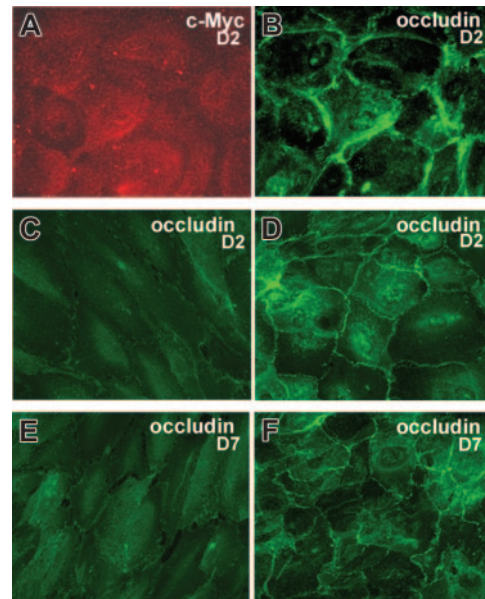


**Figure 6. Expression of DN-RhoK in BBB constructs decreases monocyte migration.** TJ alterations in BMVECs after transfection with DA-RhoK or DN-RhoK tagged with c-Myc. Transfection with DN-RhoK was confirmed by c-Myc expression (A) and resulted in the up-regulation of occludin in TJs ([B,D] 2 days after transfection; [F] 7 days after transfection). BMVECs transfected with DA-RhoK show decreased occludin and the loss of intercellular contacts ([C] 2 days after transfection; [E] 7 days after transfection). Double immunolabeling for c-Myc (A) and occludin (B) and immunolabeling for occludin (D-F). Original magnification (A-B)  $\times 400$ ; (C-F)  $\times 200$ . Images were visualized using a  $40 \times 0.75$  NA objective and were acquired using a Color View II digital CCD camera. (G) BMVECs in BBB constructs were transfected with DA-RhoK and DN-RhoK. Freshly elutriated monocytes ( $10^5$ ) were applied to BBB constructs, and their migration was studied in response to MCP-1 (5 ng/mL in the lower chamber). Transfection of BMVECs with DN-Rho decreased monocyte migration across the BBB by 84%. Results were normalized to migration of uninfected monocytes without MCP-1 (a value of 100%). Values represent the mean of quadruplicate determinations  $\pm$  SEM.

undergoes phosphorylation in vivo during monocyte migration across the BBB.

To investigate the role of RhoK in monocyte migration, we applied Y-27632 (10  $\mu$ M) to BBB constructs for 2 hours. Before the addition of monocytes to the upper chamber, the constructs were washed. Alternatively, replicate monocytes were pretreated with Y-27632 for 2 hours before application to BBB models. Again, MCP-1 (applied to the lower chamber) increased monocyte migration (5-fold,  $P < .001$ ). Pretreatment of endothelial cells with Y-27632 resulted in 90% inhibition of cell migration ( $P < .001$ ), and treatment of monocytes with Y-27632 diminished cell passage by 85% ( $P < .01$ , Figure 7I). While Ashida and colleagues<sup>44</sup> demonstrated the effect of RhoK inhibition in monocytes on their migration, our results, for the first time, prove that RhoK suppression in endothelial cells may play an equally important role in the

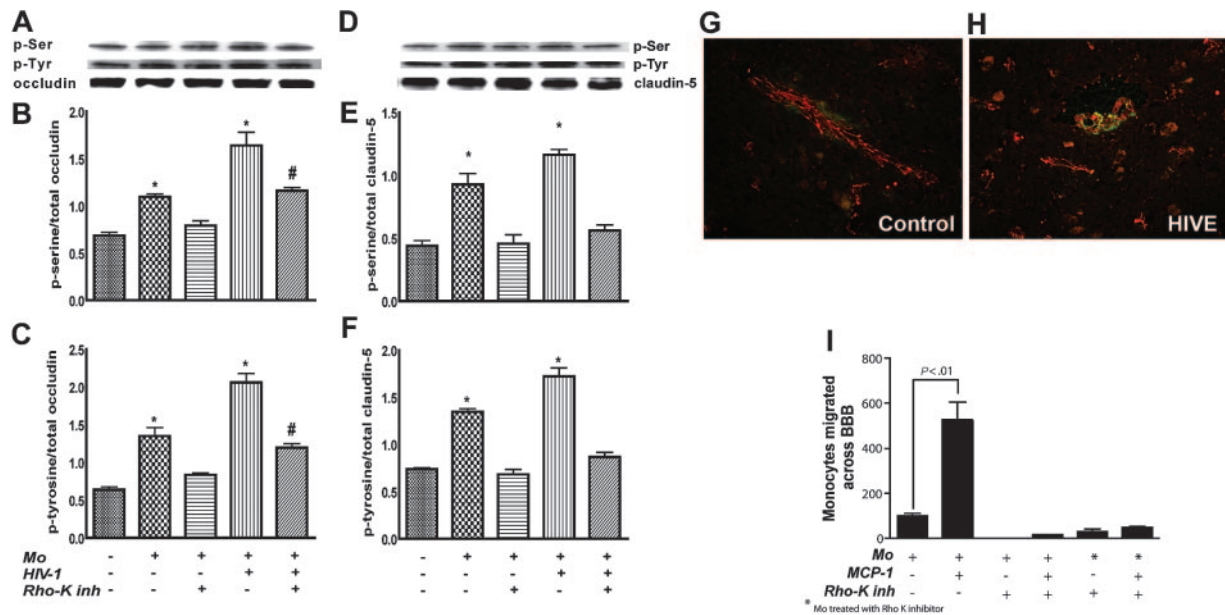


**Figure 7. Activation of Rho in BMVECs by monocytes leads to phosphorylation of TJ proteins, and RhoK inhibitor (Y-27632) blocks monocyte migration across the BBB.** The content of phosphorylated occludin and total occludin was measured in endothelial cells, endothelial cells cocultured with monocytes, and monocytes cocultured with endothelial cells after pretreatment with the RhoK inhibitor (Y-27632). (A) Representative immunoblots of phosphorylated occludin/claudin-5, total occludin/claudin-5, and internal standard, actin. (B) Ratio of phosphorylated occludin-actin (phosphoserine). (C) Ratio of phosphorylated occludin-actin (phosphotyrosine). (D) Representative immunoblots of phosphorylated claudin-5, total claudin-5, and internal standard, actin. (E) Ratio of phosphorylated claudin-5-actin (phosphoserine). (F) Ratio of phosphorylated claudin-5-actin (phosphotyrosine). Each bar represents mean value  $\pm$  SEM ( $n = 4$ ). (G-H) Human brain sections were double immunostained with antibodies to occludin/phosphoserine. While no immunostaining for phosphoserine was found in control brain tissue (G), phosphoserine staining (green) partially overlapped with occludin (red) on brain microvessels in HIV (H). (G-H) Original magnification,  $\times 400$ . Images were visualized using a  $40 \times /0.75$  NA objective and were acquired using a Color View II digital CCD camera. (I) Monocyte migration ( $10^5$  monocytes applied to BBB constructs) was studied in response to MCP-1 (5 ng/mL in the bottom chamber). Pretreatment of endothelial cells in the top chamber or monocytes (before application to top chamber\*) with RhoK inhibitor, Y-27632 (2 hours; 10  $\mu$ M), diminished monocyte migration across the BBB by 90% and 85%, respectively. Results were normalized to migration of uninfected monocytes without MCP-1 (a value of 100%). Values represent mean of quadruplicate determinations  $\pm$  SEM.

prevention of monocyte migration across BMVECs. Immunostaining for occludin demonstrated preservation of TJs along the cellular borders after treatment with Y-27632 (data not shown).

It was shown that occludin and claudin-5 phosphorylation is associated with increased permeability and decreased “tightness” of the BBB.<sup>34,45</sup> To correlate the pattern of monocyte migration with functional changes of TJs, we measured TEER paralleling monocyte migration across BBB models. Application of monocytes to the upper chamber of the BBB resulted in diminished TEER (87% by 0.5 hours and 14.5% by 1 hour,  $P < .001$ ) as compared with the BBB without monocytes (Figure 8A). Such decreases reflected the rate of monocyte migration at 0.5 and 1 hour (Figure 8B). MCP-1 introduction to the lower chamber resulted in greater TEER diminution (13.5% by 0.5 hours,  $P < .001$ ) and mirrored the increased monocyte penetration across the endothelial monolayer in response to the MCP-1 chemotactic gradient (Figure 8). A 9.1% decrease in TEER was detected at 1 hour after monocyte application in the presence of MCP-1. At this time, most monocytes had crossed the BBB and were detected in the lower chamber at levels that were 3-fold greater than levels of monocytes from BBB without MCP-1 (Figure 8B). Such changes in TEER suggest that monocytes crossing the endothelial monolayer are responsible for diminished barrier “tightness.” Importantly, pretreatment of endothelial cells with RhoK inhibitor diminished both monocyte migration ( $P < .05$ ) and prevented a decrease in TEER ( $P > .05$ ) for all conditions except monocyte/MCP-1 ( $P = .045$ ) 0.5 hours after monocyte application. Taken together, these observations provide direct evidence that inhibition of Rho/RhoK activity in BMVECs caused by monocytes preserves TJ function and diminishes monocyte migration across the BBB.

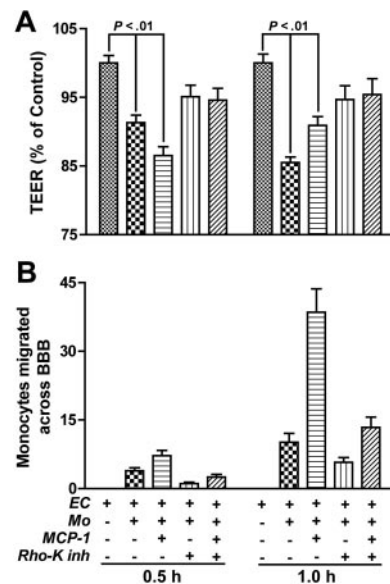


**Figure 8. Pretreatment of endothelial cells with RhoK inhibitor diminishes monocyte migration and prevents TEER decrease.** (A) TEER was investigated after application of  $10^5$  monocytes to the BBB (with or without addition of MCP-1 to the lower chamber). Application of monocytes (0.5 and 1 hours) resulted in a significant decrease of TEER that paralleled the rate of monocyte migration into the lower chamber (B). Pretreatment of endothelial cells in the upper chamber with RhoK inhibitor, Y-27632 (2 hours; 10  $\mu$ M), attenuated the TEER decrease and diminished monocyte migration across the BBB. TEER results (A) were normalized to measurements in the BBB without monocytes (a value of 100%). Migrated monocytes (immunostained with CD68) were counted in 20 random fields (objective,  $\times 20$ ) in each well. Values represent mean of quadruplicate determinations  $\pm$  SEM.

## Discussion

The BBB is compromised in HAD<sup>46</sup>; however, the mechanism causing its dysfunction is not well understood.<sup>13</sup> Small GTP-binding proteins such as Rho have been proposed to play a role in endothelial-cell TJ assembly through activation of signaling pathways that regulate cytoskeletal organization.<sup>47</sup> We hypothesize that TJ compromise is associated with Rho activation in BMVECs and is mediated by monocyte brain migration during HIVE. In the current report we demonstrated that monocytes attach to BMVEC borders (connected by TJs) and migration occurs through the cleft between adjacent endothelial cells; monocyte–endothelial-cell interactions result in Rho activation and occludin/cludin-5 phosphorylation; inhibition of Rho and RhoK in BMVECs decreases monocyte migration; BMVEC transfection with DN-RhoK leads to up-regulation of TJs and a decrease of monocyte migration; and a decrease of BBB integrity and occludin/cludin-5 phosphorylation are prevented by RhoK inhibitor.

Monocyte migration between brain endothelial-cell borders in response to MCP-1 was documented in our BBB system. SEM showed monocyte attachment to BMVEC contacts containing TJs and migration through the cleft between adjacent endothelial cells. Schenkel et al<sup>48</sup> recently demonstrated that monocytes move in an orderly fashion to the nearest junction between endothelial cells before migration. Our analyses of human brain tissue with HIVE suggested that migration occurs between endothelial-cell borders, and TJ disruption correlated with the intensity of monocyte infiltration (numbers of migrated cells). A direct link between Rho activation and TJ disruption was established in the BBB model, where the application of monocytes to the brain endothelial monolayer resulted in Rho activation and phosphorylation of the TJ proteins, occludin and claudin-5. Association of occludin phosphorylation and increased permeability of endothelial monolayers were previously demonstrated,<sup>45,49,50</sup> whereas occludin dephosphorylation in retinal endothelial cells after exposure to dexamethasone resulted in tightening of the barrier.<sup>51</sup> We found that pretreatment of BBB constructs with Rho inhibitor blocked the migration of both HIV-1-infected and uninfected cells. The role of Rho signaling pathways in BMVEC TJ assembly was further demonstrated by transient transfection of primary human BMVECs with DA-RhoK or DN-RhoK. When DN-RhoK–transfected BMVECs were used to assemble BBB constructs, a reduction in monocyte passage across the BBB in response to MCP-1 was shown. Transfection with DA-RhoK resulted in the dislocation of occludin from the membrane and the loss of intercellular contacts, similar to results previously demonstrated with dominant-active Rho.<sup>52</sup> Pretreatment of endothelial cells in BBB models with a specific RhoK inhibitor resulted in 90% diminution of monocyte migration, prevented TJ phosphorylation, and ameliorated a decrease of BBB tightness associated with monocyte migration. These observations provide direct evidence that Rho/RhoK in BMVECs plays a role in TJ function and monocyte migration across the BBB. Our future experiments will determine phosphorylation sites of occludin and claudin-5.

Significant evidence exist that the Rho family of small GTPases controls junctional complex assembly in epithelial and endothelial cells.<sup>50,53</sup> G proteins are key mediators of actin cytoskeletal remodeling, formation of cell-cell and cell-substrate adhesions, cell migration, and adhesion.<sup>54</sup> The best-characterized effectors of Rho include RhoK, which is involved in the regulation of actin organization, cellular morphology, and cellular transforma-

tion.<sup>26,55,56</sup> A number of studies demonstrated Rho participation in endothelial-cell function. Clear evidence for Rho protein involvement in tumor necrosis factor- $\alpha$  (TNF- $\alpha$ )–related signal transduction has been shown in human umbilical vein endothelial cells (HUVECs) where intracellular microinjection of the Rho inhibitor, C3 transferase, prevented TNF- $\alpha$ –induced cell retraction and formation of intercellular gaps.<sup>57</sup> Another study demonstrated that inactivation of endothelial Rho by *Clostridium limosum* exoenzyme C (acting in a fashion similar to C3 transferase) results in a reduced rate of monocyte transmigration through a monolayer of dermal microvascular endothelial cells devoid of TJs.<sup>58</sup> In terms of mechanism, the authors speculated that Rho may stabilize the cytoskeleton, because absence of stress fiber formation was demonstrated by F-actin staining. Absence of chemokine gradients in their system (usually present in any inflammatory condition) makes this study inconclusive. Saito and colleagues<sup>59</sup> studied neutrophil migration across HUVEC monolayers, demonstrating that pretreating endothelial cells with Rho or RhoK inhibitors diminished neutrophil migration, actin polymerization, and myosin II filament formation. These data suggest that endothelial Rho and RhoK regulate transendothelial neutrophil migration by modulating the cytoskeletal events. Stamatovic and colleagues<sup>31,60</sup> demonstrated that Rho/RhoK is involved in redistribution of TJ proteins and increased permeability of monolayer of mouse brain endothelial cells treated with MCP-1.

The importance of Rho in leukocyte migration across endothelium was demonstrated through crosslinking of intercellular adhesion molecule-1 (ICAM-1) (mimicking leukocyte–endothelial-cell interactions), which resulted in Rho-dependent cytoskeleton reorganization in BMVECs, and barrier disruption.<sup>61</sup> Inhibition of Rho prevented clustering of adhesion molecules (ICAM-1, VCAM-1, and E selectin) and decreased monocyte adhesion to endothelial cells.<sup>62</sup> Application of the Rho inhibitor to BMVECs significantly decreased T-lymphocyte migration and endothelial actin reorganization without affecting lymphocyte BMVEC adhesion.<sup>63</sup> Together, these studies demonstrate that endothelial cells are actively involved in facilitating leukocyte migration through the BBB and that this process involves functional Rho proteins.<sup>64</sup> However, the precise role of Rho in endothelial TJ regulation during leukocyte migration is currently unknown.

Several groups independently showed that leukocyte adhesion to endothelial cells is required for degradation of junctional components via signaling mechanisms that enhance leukocyte migration and monolayer permeability.<sup>65–67</sup> Shaw and colleagues demonstrated that transmigrating monocytes cause a focal and reversible disruption/dispersion of the adherent junctions (cadherin complex) in HUVECs.<sup>68</sup> The authors speculated that transmigration is a sequential multistep process that involves active participation of both leukocytes and the endothelium, similar to the multistep adhesion cascade model. Wittchen and colleagues<sup>69</sup> presented evidence of an association between enhanced TJ expression, increased tightness of the endothelial-cell monolayer, and decreased leukocyte migration across it. Exact intracellular signals and their integration with functional changes of both cell types will require further studies. The present study further extends previous observations suggesting that Rho/RhoK in BMVECs play a role in TJ disassembly and monocyte migration across the BBB.

A number of studies, including the current report, support the idea that leukocyte-induced changes in endothelial-cell TJ and cytoskeletal organization facilitate leukocyte migration. Adhesion molecules, such as E selectin, VCAM-1, and ICAM-1 were

proposed as the key molecules that affect the signal transduction pathway in endothelial cells and induce the functional changes of endothelial cells in the interaction with leukocytes.<sup>62</sup> We showed before that these adhesion molecules were up-regulated on BMVECs in HIVE<sup>70</sup> and on the BBB model during migration of virus-infected and activated macrophages.<sup>32</sup> Dallasta and colleagues demonstrated significant TJ disruption (as indicated by diminished ZO-1 and occludin staining) in HIVE patients.<sup>14</sup> Based upon previous works, we propose the following scenario of BBB injury during HIVE: soluble factors and/or interactions with inflammatory cells up-regulate adhesion molecules on BMVECs<sup>32,70</sup>; monocytes are activated in peripheral blood<sup>14,5,71</sup> and attracted to the BBB by increased secretion of  $\beta$ -chemokines within the CNS<sup>33,72</sup>; and monocyte-BMVEC interactions lead to Rho/RhoK activation, TJ disassembly, BBB compromise, and monocyte passage into the CNS. This process is most probably operational under physiologic conditions (turnover of perivascular macrophages) and during neuroinflammatory states (like HIVE). Because the latter is accompanied by more massive leukocyte migration in the presence of chemokine gradient, TJ alterations are more prominent resulting in BBB increased permeability to serum proteins and toxic factors present in peripheral circulation.

Our results indicate an important role of endothelial Rho/RhoK in regulating HIV-1-infected monocytes across the BBB. Because it is well established that the best histopathologic correlate of HAD is the number of activated monocytes/macrophages in the CNS<sup>3</sup> that are shown to migrate from the peripheral blood,<sup>71,73</sup> therapeutic strategies that inhibit processes of monocyte/macrophage transendothelial migration may thus be useful as an adjunctive therapy for HAD.

## Acknowledgments

We thank Ms Robin Taylor for excellent administrative support; David Erichsen, Casey Diekmann, and Bryan Knipe for technical support; and Drs Howard E. Gendelman and Lee Mosley for critical reading of the manuscript. Primary human BMVECs were provided by Drs Marlys H. Witte and Martin Weinand (Department of Surgery) through contracts with the University of Arizona Medical Center (Tucson). The National Institutes of Health (NIH) National NeuroAIDS Consortium and the Center for Neurovirology and Neurodegenerative Disorders (CNND) brain bank are acknowledged for brain tissue specimens used in this study.

## References

- Maschke M, Kastrop O, Esser S, Ross B, Hengge U, Hufnagel A. Incidence and prevalence of neurological disorders associated with HIV since the introduction of highly active antiretroviral therapy (HAART). *J Neurol Neurosurg Psychiatry*. 2000; 69:376-380.
- Masliyah E, DeTeresa RM, Mallory ME, Hansen LA. Changes in pathological findings at autopsy in AIDS cases for the last 15 years. *AIDS*. 2000; 14:69-74.
- Glass J, Fedor H, Wesselingh S, McArthur J. Immunocytochemical quantitation of human immunodeficiency virus in the brain: correlations with dementia. *Ann Neurol*. 1995;38:755-762.
- Williams KC, Corey S, Westmoreland SV, et al. Perivascular macrophages are the primary cell type productively infected by simian immunodeficiency virus in the brains of macaques: implications for the neuropathogenesis of AIDS. *J Exp Med*. 2001;193:905-915.
- Williams K, Westmoreland S, Greco J, et al. Magnetic resonance spectroscopy reveals that activated monocytes contribute to neuronal injury in SIV neuroAIDS. *J Clin Invest*. 2005;115:2534-2545.
- Genis P, Jett M, Bernton E, Boyle T, et al. Cytokines and arachidonic metabolites produced during human immunodeficiency virus (HIV)-infected macrophage-astroglia interactions: implications for the neuropathogenesis of HIV disease. *J Exp Med*. 1992;176:1703-1718.
- Nottet HS, Jett M, Flanagan CR, Zhai QH, et al. A regulatory role for astrocytes in HIV-1 encephalitis: an overexpression of eicosanoids, platelet-activating factor, and tumor necrosis factor- $\alpha$  by activated HIV-1-infected monocytes is attenuated by primary human astrocytes. *J Immunol*. 1995;154:3567-3581.
- Gelbard H, Nottet H, Swindells S, et al. Platelet-activating factor: a candidate human immunodeficiency virus type 1-induced neurotoxin. *J Virol*. 1994;68:4628-4635.
- Heyes MP, Ellis RJ, Ryan L, et al. Elevated cerebrospinal fluid quinolinic acid levels are associated with region-specific cerebral volume loss in HIV infection. *Brain*. 2001;124:1033-1042.
- Adamson D, Wildemann B, Sasaki M, et al. Immunologic NO synthase: elevation in severe AIDS dementia and induction by HIV-1 gp41. *Science*. 1996;274:1917-1921.
- Ghorpade A, Persidskaia R, Suryadevara R, et al. Mononuclear phagocyte differentiation, activation, and viral infection regulate matrix metalloproteinase expression: implications for human immunodeficiency virus type 1-associated dementia. *J Virol*. 2001;75:6572-6583.
- Brenneman DE, Westbrook GL, Fitzgerald SP, et al. Neuronal cell killing by the envelope protein of HIV and its prevention by vasoactive intestinal peptide. *Nature (Lond)*. 1988;335:639-642.
- Persidsky Y, Gendelman HE. Mononuclear phagocyte immunity and the neuropathogenesis of HIV-1 infection. *J Leukoc Biol*. 2003;74:691-701.
- Dallasta LM, Pisarov LA, Esplen JE, et al. Blood-brain barrier tight junction disruption in human immunodeficiency virus-1 encephalitis. *Am J Pathol*. 1999;155:1915-1927.
- Persidsky Y, Zheng J, Miller D, Gendelman HE. Mononuclear phagocytes mediate blood-brain barrier compromise and neuronal injury during HIV-1-associated dementia. *J Leukoc Biol*. 2000; 68:413-422.
- Gendelman HE, Zheng J, Coulter CL, et al. Suppression of inflammatory neurotoxins by highly active antiretroviral therapy in human immunodeficiency virus-associated dementia. *J Infect Dis*. 1998;178:1000-1007.
- Avison MJ, Nath A, Greene-Avison R, Schmitt FA, Greenberg RN, Berger JR. Neuroimaging correlates of HIV-associated BBB compromise. *J Neuroimmunol*. 2004;157:140-146.
- Pardridge WM. Brain metabolism: a perspective from the blood-brain barrier. *Physiol Rev*. 1983; 63:1481-1535.
- Morita K, Sasaki H, Furuse M, Tsukita S. Endothelial claudin: claudin-5/TMVCV constitutes tight junction strands in endothelial cells. *J Cell Biol*. 1999;147:185-194.
- Rubin LL, Staddon JM. The cell biology of the blood-brain barrier. *Annu Rev Neurosci*. 1999;22: 11-28.
- Nitta T, Hata M, Gotoh S, et al. Size-selective loosening of the blood-brain barrier in claudin-5-deficient mice. *J Cell Biol*. 2003;161:653-660.
- Morita K, Sasaki H, Furuse K, Furuse M, Tsukita S, Miyachi Y. Expression of claudin-5 in dermal vascular endothelia. *Exp Dermatol*. 2003;12:289-295.
- Stevenson BR. Understanding tight junction clinical physiology at the molecular level. *J Clin Invest*. 1999;104:3-4.
- Schnitler HJ. Structural and functional aspects of intercellular junctions in vascular endothelium. *Basic Res Cardiol*. 1998;93:30-39.
- Fanning AS, Jameson BJ, Jesaitis LA, Anderson JM. The tight junction protein ZO-1 establishes a link between the transmembrane protein occludin and the actin cytoskeleton. *J Biol Chem*. 1998; 273:29745-29753.
- Itoh K, Yoshioka K, Akedo H, Uehata M, Ishizaki T, Narumiya S. An essential part for Rho-associated kinase in the transcellular invasion of tumor cells. *Nat Med*. 1999;5:221-225.
- Yang L, Froio RM, Sciuto TE, Dvorak AM, Alon R, Luscinskas FW. ICAM-1 regulates neutrophil adhesion and transcellular migration of TNF- $\alpha$ -activated vascular endothelium under flow. *Blood*. 2005;106:584-592.
- Muller WA. Leukocyte-endothelial-cell interactions in leukocyte transmigration and the inflammatory response. *Trends Immunol*. 2003;24:327-334.
- Luscinskas FW, Ma S, Nusrat A, Parkos CA, Shaw SK. The role of endothelial cell lateral junctions during leukocyte trafficking. *Immunol Rev*. 2002;186:57-67.
- Luscinskas FW, Ma S, Nusrat A, Parkos CA, Shaw SK. Leukocyte transendothelial migration: a junctional affair. *Semin Immunol*. 2002;14:105-113.
- Stamatovic SM, Keep RF, Kunkel SL, Andjelkovic AV. Potential role of MCP-1 in endothelial cell tight junction 'opening': signaling via Rho and Rho kinase. *J Cell Sci*. 2003;116:4615-4628.
- Persidsky Y, Stins M, Way D, et al. A model for monocyte migration through the blood-brain barrier during HIV-1 encephalitis. *J Immunol*. 1997; 158:3499-3510.
- Persidsky Y, Ghorpade A, Rasmussen J, et al. Microglial and astrocyte chemokines regulate monocyte migration through blood-brain barrier in human immunodeficiency virus-1 encephalitis. *Am J Pathol*. 1999;155:1599-1611.
- Haorah J, Knipe B, Leibhart J, Ghorpade A, Persidsky Y. Alcohol-induced oxidative stress in brain endothelial cells causes blood-brain barrier dysfunction. *J Leukoc Biol*. 2005;78:1223-1232.

35. Gendelman HE, Orenstein JM, Martin MA, et al. Efficient isolation and propagation of human immunodeficiency virus on recombinant colony-stimulating factor 1-treated monocytes. *J Exp Med.* 1988;167:1428-1441.
36. Ghorpade A, Nukuna A, Che M, et al. Human immunodeficiency virus neurotropism: an analysis of viral replication and cytopathicity for divergent strains in monocytes and microglia. *J Virol.* 1998;72:3340-3350.
37. Oshiro N, Fukata Y, Kaibuchi K. Phosphorylation of moesin by rho-associated kinase (Rho-kinase) plays a crucial role in the formation of microvilli-like structures. *J Biol Chem.* 1998;273:34663-34666.
38. Morishige K, Shimokawa H, Eto Y, et al. Adenovirus-mediated transfer of dominant-negative rho-kinase induces a regression of coronary arteriosclerosis in pigs in vivo. *Arterioscler Thromb Vasc Biol.* 2001;21:548-554.
39. Ikezu T, Luo X, Weber GA, et al. Amyloid precursor protein-processing products affect mononuclear phagocyte activation: pathways for sAPP- and Abeta-mediated neurotoxicity. *J Neurochem.* 2003;85:925-934.
40. Potula R, Poluektova L, Knipe B, et al. Inhibition of indoleamine 2,3-dioxygenase (IDO) enhances elimination of virus-infected macrophages in an animal model of HIV-1 encephalitis. *Blood.* 2005;106:2382-2390.
41. Pomorski P, Watson JM, Haskill S, Jacobson KA. How adhesion, migration, and cytoplasmic calcium transients influence interleukin-1beta mRNA stabilization in human monocytes. *Cell Motil Cytoskeleton.* 2004;57:143-157.
42. Kaibuchi K, Kuroda S, Amano M. Regulation of the cytoskeleton and cell adhesion by the Rho family GTPases in mammalian cells. *Annu Rev Biochem.* 1999;68:459-486.
43. Wojciak-Stothard B, Potempa S, Eichholtz T, Ridley AJ. Rho and Rac but not Cdc42 regulate endothelial cell permeability. *J Cell Sci.* 2001;114:1343-1355.
44. Ashida N, Arai H, Yamasaki M, Kita T. Distinct signaling pathways for MCP-1-dependent integrin activation and chemotaxis. *J Biol Chem.* 2001;276:16555-16560.
45. Hirase T, Kawashima S, Wong E, et al. Regulation of tight junction permeability and occludin phosphorylation by RhoA-p160ROCK-dependent and -independent mechanisms. *J Biol Chem.* 2001;276:10423-10431.
46. Weis S, Haug H, Budka H. Vascular changes in the cerebral cortex in HIV-1 infection, I: a morphometric investigation by light and electron microscopy. *Clin Neuropathol.* 1996;15:361-366.
47. Moon SY, Zheng Y. Rho GTPase-activating proteins in cell regulation. *Trends Cell Biol.* 2003;13:13-22.
48. Schenkel AR, Mamdouh Z, Muller WA. Locomotion of monocytes on endothelium is a critical step during extravasation. *Nat Immunol.* 2004;5:393-400.
49. Antonetti DA, Barber AJ, Hollinger LA, Wolpert EB, Gardner TW. Vascular endothelial growth factor induces rapid phosphorylation of tight junction proteins occludin and zonula occluden 1: a potential mechanism for vascular permeability in diabetic retinopathy and tumors. *J Biol Chem.* 1999;274:23463-23467.
50. Feldman GJ, Mullin JM, Ryan MP. Occludin: structure, function and regulation. *Adv Drug Deliv Rev.* 2005;57:883-917.
51. Antonetti DA, Wolpert EB, DeMaio L, Harhaj NS, Scaduto RC Jr. Hydrocortisone decreases retinal endothelial cell water and solute flux coincident with increased content and decreased phosphorylation of occludin. *J Neurochem.* 2002;80:667-677.
52. Bruewer M, Hopkins AM, Hobert ME, Nusrat A, Madara JL. RhoA, Rac1, and Cdc42 exert distinct effects on epithelial barrier via selective structural and biochemical modulation of junctional proteins and F-actin. *Am J Physiol Cell Physiol.* 2004;287:C327-C335.
53. Madara JL. Regulation of the movement of solutes across tight junctions. *Annu Rev Physiol.* 1998;60:143-159.
54. Hopkins AM, Li D, Mrsny RJ, Walsh SV, Nusrat A. Modulation of tight junction function by G protein-coupled events. *Adv Drug Deliv Rev.* 2000;41:329-340.
55. Amano M, Chihara K, Kimura K, et al. Formation of actin stress fibers and focal adhesions enhanced by Rho-kinase. *Science.* 1997;275:1308-1311.
56. Leung T, Manser E, Tan L, Lim L. A novel serine/threonine kinase binding the Ras-related RhoA GTPase which translocates the kinase to peripheral membranes. *J Biol Chem.* 1995;270:29051-29054.
57. Wojciak-Stothard B, Entwistle A, Garg R, Ridley AJ. Regulation of TNF-alpha-induced reorganization of the actin cytoskeleton and cell-cell junctions by Rho, Rac, and Cdc42 in human endothelial cells. *J Cell Physiol.* 1998;176:150-165.
58. Strey A, Janning A, Barth H, Gerke V. Endothelial Rho signaling is required for monocyte transendothelial migration. *FEBS Lett.* 2002;517:261-266.
59. Saito H, Minamiya Y, Saito S, Ogawa J. Endothelial Rho and Rho kinase regulate neutrophil migration via endothelial myosin light chain phosphorylation. *J Leukoc Biol.* 2002;72:829-836.
60. Stamatovic SM, Shakui P, Keep RF, et al. Monocyte chemoattractant protein-1 regulation of blood-brain barrier permeability. *J Cereb Blood Flow Metab.* 2005;25:593-606.
61. Etienne S, Adamson P, Greenwood J, Strosberg AD, Cazaubon S, Couraud PO. ICAM-1 signaling pathways associated with Rho activation in microvascular brain endothelial cells. *J Immunol.* 1998;161:5755-5761.
62. Wojciak-Stothard B, Williams L, Ridley AJ. Monocyte adhesion and spreading on human endothelial cells is dependent on Rho-regulated receptor clustering. *J Cell Biol.* 1999;145:1293-1307.
63. Adamson P, Etienne S, Couraud PO, Calder V, Greenwood J. Lymphocyte migration through brain endothelial cell monolayers involves signaling through endothelial ICAM-1 via a rho-dependent pathway. *J Immunol.* 1999;162:2964-2973.
64. Wittchen ES, van Buul JD, Burrigge K, Worthylake RA. Trading spaces: Rap, Rac, and Rho as architects of transendothelial migration. *Curr Opin Hematol.* 2005;12:14-21.
65. Del Maschio A, Zanetti A, Corada M, et al. Polymorphonuclear leukocyte adhesion triggers the disorganization of endothelial cell-to-cell adherens junctions. *J Cell Biol.* 1996;135:497-510.
66. Allport JR, Muller WA, Luscinskas FW. Monocytes induce reversible focal changes in vascular endothelial cadherin complex during transendothelial migration under flow. *J Cell Biol.* 2000;148:203-216.
67. Xu H, Dawson R, Crane IJ, Liversidge J. Leukocyte diapedesis in vivo induces transient loss of tight junction protein at the blood-retina barrier. *Invest Ophthalmol Vis Sci.* 2005;46:2487-2494.
68. Shaw SK, Bamba PS, Perkins BN, Luscinskas FW. Real-time imaging of vascular endothelial-cadherin during leukocyte transmigration across endothelium. *J Immunol.* 2001;167:2323-2330.
69. Wittchen ES, Worthylake RA, Kelly P, Casey PJ, Quilliam LA, Burrigge K. Rap1 GTPase inhibits leukocyte transmigration by promoting endothelial barrier function. *J Biol Chem.* 2005;280:11675-11682.
70. Nottet HS, Persidsky Y, Sasseville VG, et al. Mechanisms for the transendothelial migration of HIV-1-infected monocytes into brain. *J Immunol.* 1996;156:1284-1295.
71. Pulliam L, Gascon R, Stubblebine M, McGuire D, McGrath MS. Unique monocyte subset in patients with AIDS dementia. *Lancet.* 1997;349:692-695.
72. Conant K, Garzino-Demo A, Nath A, et al. Induction of monocyte chemoattractant protein-1 in HIV-1 Tat-stimulated astrocytes and elevation in AIDS dementia. *Proc Natl Acad Sci U S A.* 1998;95:3117-3121.
73. Sanchez-Ramon S, Bellon JM, Resino S, et al. Low blood CD8+ T-lymphocytes and high circulating monocytes are predictors of HIV-1-associated progressive encephalopathy in children. *Pediatrics.* 2003;111:E168-E175.



**blood**<sup>®</sup>

2006 107: 4770-4780

doi:10.1182/blood-2005-11-4721 originally published online  
February 14, 2006

## **Rho-mediated regulation of tight junctions during monocyte migration across the blood-brain barrier in HIV-1 encephalitis (HIVE)**

Yuri Persidsky, David Heilman, James Haorah, Marina Zelivyanskaya, Raisa Persidsky, Gregory A. Weber, Hiroaki Shimokawa, Kozo Kaibuchi and Tsuneya Ikezu

---

Updated information and services can be found at:

<http://www.bloodjournal.org/content/107/12/4770.full.html>

Articles on similar topics can be found in the following Blood collections

[Cell Adhesion and Motility](#) (790 articles)

[Cytoskeleton](#) (143 articles)

[Immunobiology](#) (5457 articles)

[Phagocytes](#) (969 articles)

[Signal Transduction](#) (1930 articles)

---

Information about reproducing this article in parts or in its entirety may be found online at:

[http://www.bloodjournal.org/site/misc/rights.xhtml#repub\\_requests](http://www.bloodjournal.org/site/misc/rights.xhtml#repub_requests)

Information about ordering reprints may be found online at:

<http://www.bloodjournal.org/site/misc/rights.xhtml#reprints>

Information about subscriptions and ASH membership may be found online at:

<http://www.bloodjournal.org/site/subscriptions/index.xhtml>